DRAFT
9/22/97

ELECTRON BEAM TREATMENT HEAD

by
Kenneth R. Hogstrom, Ph.D.
Department of Radiation Physics
The University of Texas M. D. Anderson Cancer Center
Houston, TX

I. Introduction

The treatment head of a radiotherapy accelerator is configured to provide an electron or x-ray beam suitable for patient radiotherapy. This paper will discuss the functional components necessary for a clinical electron beam. In most conventional radiotherapy accelerators, the electron beam exits the linear accelerator approximately as a point, monoenergetic, monodirectional beam, traveling parallel to the isocentric axis of the gantry approximately 1 m away. Since the patient is typically lying along the isocentric axis, it is the objective of the treatment head to redirect, broaden, collimate, and monitor the beam. This should result in a uniform, shaped beam of known output (dose per monitor unit) to be approximately perpendicularly incident on the patient.

II. Bending Magnet

The purpose of the bending magnet is to redirect the incident point electron beam by 90° such that it remains a point, monodirectional beam, even though the incident beam has a small energy spread (ΔE). This requires what is referred to as an achromatic (or sometimes doubly achromatic) system. This has been explained in some detail by Karzmark (1984) and Karzmark et al. (1993) will be summarized here. Figure 1a illustrates a 90° bending magnet which has energy dispersion, that is the higher energy electrons $E+\Delta E$ get bent less than the lower energy electrons $E-\Delta E$, resulting in the point beam being spatially spread after exiting the magnet. Figure 1b illustrates a 270° bending magnet which focuses all electrons to a point, but an energy-angle correlation remains. This would ultimately result in the electron beam reaching the patient having a position-dependent penetration (e.g. R_{90}). Figure 2a illustrates an achromatic system in which all electrons return to the same point traveling in the same direction, regardless of incident energy. This effect is accomplished by placing a gradient in the magnetic field by varying the pole separation as illustrated in Figure 2b. Figure 3 shows the type of 270° achromatic bending magnet employed by Siemens Mevatrons; systems used by other manufacturers are described by Karzmark et al. (1993).

The central orbit of the magnet has a characteristic radius of curvature (ρ), which must be kept small otherwise the treatment head becomes too bulky, which necessitates an increased isocenter height. The momentum (p) of the electron beam is related to the magnet parameters by $p=eB\rho$, where e is the electron charge and B is the strength of the magnetic field. Each electron energy ($E=pc$) requires a unique magnetic

field B. For example, a 15 kG dipole field will bend a 25-MeV electron beam with a radius of 5.66 cm. For the same radius of curvature, a 5-MeV electron beam requires a field of only 3.24 kG. The bending magnet is an electromagnet, whose magnetic field is governed by the current (I) passing through its coils. However, because of iron hysteresis and saturation effects, a programmed sequence of magnet current changes may be required to accurately reproduce a specific beam energy.

Bending of the electrons normally takes place in a vacuum contiguous with that of the accelerator. Hence, when the electron beam exits the bending magnet system, any energy spread in the beam is that due to the accelerator and that caused by energy loss straggling in the vacuum window. Typically, the vacuum window is located just beyond 100 cm from isocenter.

III. Broadening the Electron Beam

Once exiting the bending magnet, a specific electron beam energy has been selected, and the beam is directed towards isocenter (the patient). The next function of the treatment head is to broaden the beam. This typically requires that the beam be uniform for field sizes as large as 25×25 cm^2 to 30×30 cm^2. This is accomplished by either a scattering foil or magnetic beam scanning system.

A. Scatter Foil System

The primary scattering foil is typically a thin, high-Z foil located within a few centimeters of the end window. Its location varies with manufacturer, depending on the mechanical design for selecting x-ray targets and electron scattering foils. A high-Z foil is utilized because it can give the greatest amount of scattering with the least energy loss. The primary scattering foil has a small cross-section (<1 cm diameter), as the size of the electron beam is usually on the order of a millimeter. After exiting the foil, the electron beam has a Gaussian angular distribution, which results in a Gaussian spatial distribution at isocenter. Scattering by the intervening air and the transmission ionization chamber is relatively insignificant to that arising from the primary scattering foil and vacuum window. Figure 4 illustrates the resulting radial profile of relative electron fluence. This method of beam flattening is extremely inefficient, as only the central region of the Gaussian with an off-axis ration greater than 0.9 is clinically useful. Hence, single scattering foil applications are limited to small fields and low energies. The primary scattering foil is the major source of background bremsstrahlung dose (D_x) in the electron beam. Single scattering foils sufficiently thick to flatten a 25×25 cm^2 field ($r_{max} = {}^{25}/_{\sqrt{2}}$ cm) would generate an unacceptable high D_x.

This problem is solved by a dual scattering foil system, the secondary scattering foil being placed downstream of the primary foil. The secondary foil is approximately Gaussian-shaped and made of a low-Z foil (e.g. Al). The low Z results in an insignificant increase to the bremsstrahlung dose. The secondary foil establishes a lateral disequilibrium with more electrons scattering away from center than being scattered towards center, resulting in the Gaussian shape of the off-axis fluence distribution

decreasing its amplitude near central axis and increasing its amplitude away from central axis, resulting in a reasonably flat beam, illustrated in Figure 4. Achieving a sufficiently flat beam with minimal bremsstrahlung requires optimizing the composition and thickness of the primary foil, the composition and shape of the secondary foil, and the separation of the distance between them. The general design of the dual scattering foil system varies amongst manufacturers, as demonstrated in Table 1. For example, Siemens Mevatrons keep the secondary foil constant while varying the primary foil, whereas the General Electric Saturne does opposite that. In the Varian Clinac, both foils vary with energy.

	1° foil		2° foil	
Manufacturer/Model	distance from isocenter	energy dependence	separation	energy dependence
Siemens Mevatron	98 cm	variable	15 cm	fixed
Varian Clinac	90 cm	variable	5 cm	variable
General Electric Saturne	95 cm	fixed	20 cm	variable

Table 1: Design of dual scattering foil systems for various manufacturers.

The shaped secondary foil must be centered on the central axis of the radiation beam, which also must be symmetrical to have a symmetrical beam at isocenter. In the course of accelerator acceptance, it may be necessary for the accelerator technologist to adjust the lateral position of the foil to optimize symmetry. In the Varian Clinac, the primary-secondary foil separation is the closest (5 cm), making its alignment the most critical. On the other hand, because of the closeness, the primary and secondary foil are a single unit, as illustrated in Figure 5. Although adjustments can be made to correct for symmetry, flatness is governed by the dual foil system design and cannot be changed without changing foils. The dual foil system should not be changed once the machine leaves the factory. In the radiotherapy installation, following replacement of an accelerator structure or bending magnet, the electron beams should be tuned to their previous energy; under no circumstances should the dual foil system be changed. Any such change will likely require a recommissioning of all dosimetry data for that energy. Figure 6 illustrates how beam flatness changes on a Siemens Mevatron 12-MeV beam as the secondary foil changes shape. Changes in the foil system are readily reflected in the characteristics of symmetry and flatness. As shown by Davis et al. (1996), a sudden change in dose output, depth dose, and flatness allowed easy diagnosis that the primary foil had dropped out of its mount.

B. Magnetic Beam Scanning System

In magnetic scanning systems, a narrow beam which has a Gaussian profile is scanned to produce a uniform or some other desired incident fluence distribution. The unscanned fluence profile is a radially symmetric Gaussian given by $Ae^{-(r/r_0)^2}$, where A is the amplitude, and r_0 is the $1/e$ width of the Gaussian. The width of the Gaussian is primarily dependent on multiple scattering that occurs in the accelerator end window,

transmission ion chamber, and intervening air. For higher electron energies (>20 MeV), a thin primary scattering foil may be used to intentionally broaden the Gaussian. Figure 7 compares radial profiles of the AECL Therac 25 unscanned 5- and 25-MeV beams. The unscanned beam is deflected laterally by controlling the orthogonal magnetic fields which scan the beam by controlling its lateral position relative to central axis. Figure 8 shows an example of how one orthogonal magnet is before the bending magnet and the other after the bending magnet. Another configuration, used by the CGR, AECL, and GE accelerators, is to place both magnets after the bending magnet, referred to as a scanning quadrapole.

The most typical objective of the scanning magnets is to produce a uniform electron fluence at isocenter. To accomplish this, the beam is scanned over a lateral dimension that results in a uniform fluence over the diagonal of the largest field size. As seen in Figure 9a for the AECL Therac-20, the diagonal of 30×30 cm^2 field is 42 cm. The beam is scanned over approximately 60 cm because of the fuzziness at the edges of the scanning pattern.

As shown in Figure 9, scanning patterns can either be a repetitive pattern, e.g. a raster scan is done for the AECL Therac 25 (O'Brien et al., 1984) or it can be asynchronous, as is done on the AECL Therac 20. The repetitive pattern has the advantage that it can be designed to deliver a non-uniform fluence that can have application such as electron wedges or conformal therapy (ref). In taking dosimetry measurements, it is useful to have data acquisition system that can gate for one cycle. The asynchronous system is only useful for producing a uniform beam. By selecting scanning frequencies for the two orthogonal magnetic fields, such that one is not an integer multiple of the other, the scanning pattern approximates random scanning. In taking dosimetry measurements it becomes necessary to take readings for several periods. If the dosimetry system is gated by the two scanning cycles, there are optimal data acquisition times (Ertan et al., 1984).

Advantages of scanned electron beams are the depth dose (less bremsstrahlung dose and a sharper falloff, R_{10}-R_{90}), and the ability to modulate the beam intensity versus position. Disadvantages of scanned electron beams are the higher recombination in ion chamber measurements (Boag, 1982), the need for more sophisticated data acquisition systems, and the risk for overirradiation should the scanning magnet fail (Purdy et al, 1993).

IV. Collimating the Beam

Electron beams must have the ability to be collimated such that the field is customized for the specific type of treatment and individual patient. The dose distribution and output depends on the collimating system, which differ considerably.

A. Principles of Collimation

The purpose of the collimating system is to shield the patient from unwanted electron dose in such a way that minimally impairs patient setup. Electron collimators stop the electron, as opposed to photon collimators, which attenuate the beam. Electrons are directly ionizing, having a maximum range that can be determined from the linear collisional stopping process (ICRU). For lead, the thickness required in millimeters is approximately one-half of the most probable incident energy in MeV, $t(mm) = 0.5\ E_{p,o}$ (MeV) (Khan et al., 1991). For example, a 20-MeV electron beam can be stopped by 1.0 cm of lead. Collimating systems are frequently made of brass, steel, or some other high density metal that is easily machineable. Figure 10 shows a measured transmission curve in brass, which shows a thickness of 13 mm is sufficient to stop an 18-MeV electron beam. The thickness of the collimating materials is usually designed for the greatest energy of the accelerator.

The lateral extent of the collimator is designed such that the electron fluence on the inside is uniform and that the electron fluence on the outside results in acceptable leakage. This is best accomplished by ensuring that the collimator intersects the penumbra generated by the collimating edge immediately upstream, as illustrated in Figure 11. Because electrons are easily scattered by air, the final, beam-defining collimator needs to be close to the patient, which for most conventional collimating systems, is 5 cm above isocenter (the standard patient SSD). If electron collimation utilized only the x-ray jaws and the final collimator 5 cm above isocenter, the required width of the final collimator would be too large, interfering with patient setup and being too heavy. A more efficient strategy is to have a series of collimating leaves. This is illustrated by the design of the Siemens variable collimator in Figure 12 (Hogstrom et al., 1985).

B. Variable Trimmers and Applicator Systems

To keep the trimmer bars of the electron variable collimator as narrow as possible, the x-ray jaws of the accelerator must move synchronously with the trimmer bars. This is accomplished either by mechanical coupling found on the CGR, AECL, and GE line of radiotherapy accelerators or by electrical coupling found on the Siemens accelerators. The most typical type of electron collimation in clinical use is the electron applicator, in which the trimmer bars are fixed to a single field size. This requires a set of applicators (e.g. 6×6 cm^2, 10×10 cm^2, 15×15 cm^2, 20×20 cm^2, and 25×25 cm^2) to allow full range of clinical use. For each applicator, the x-ray jaws must be set to a predetermined field. This occurs automatically on all newer radiotherapy accelerators, and on older radiotherapy accelerators, it is done manually, in which case the correct setting is interlocked. Typically the x-ray jaws are set to a width of 5-10 cm greater than the field size of the applicator. For some accelerators, e.g. Siemens, this varies only with applicator size, and for others, e.g. Varian (ref), it varies with both field size and energy. Usually the x-ray jaws contributes to the beam uniformity by scattering off its face, contributing more as the size of the x-ray jaws approach the electron field size. This is illustrated in Figure 13. Electron applicators always require a system that accommodates custom secondary collimating inserts, usually custom fabricated from

Cerrobend. Figure 14 shows a Cerrobend system for the Varian Clinac 2100C. Variable electron collimators are more versatile in that in that they can form any rectangular field shape within their range (e.g. 2×2 cm^2 to 25×25 cm^2 for Siemens), but are more constrictive in that custom secondary blocking is not as easily accommodated, being achieved by a thin blocking tray (e.g. mylar) below the final collimating trimmer bars or by stacking blocks on top of the leaves using Velcro or tape to hold them into place.

C. Special Collimators

In addition to standard electron collimators, there are also the specialized electron cones, which are useful for intraoral, intraoperative, and transvaginal irradiation. Electron cones are usually designed to be in contact with and perhaps inside the patient. Being in contact with the patient results in the sharpest possible penumbra. Because the collimator is inside the patient adjacent tissues may be in contact with the external wall of the cone. In such cases, it is important that leakage is controlled and measured. As pointed out by Hogstrom et al. (1990), multiple scattering requires the wall thickness of cones to be significantly greater than expected. Another property of cones is that electrons are easily scattered from the collimator wall back into the beam, an effect known as "streaming." This results in regions of increased dose, called "horns" just inside the perimeter of the radiation fields. There horns may be removed by placement of a thin ring on the inside of the cone (Hogstrom et al., 1990).

Another type of specialized electron collimation is the secondary collimator used in electron arc therapy (Hogstrom and Leavitt, 1987). In such cases the secondary collimator serves two purposes: (1) to serve as part of the collimation system and (2) to increase or decrease fluence so that the resulting dose distribution remains uniform as the radius of curvature of the patient surface from isocenter changes. The electron arc secondary collimator is usually 35-45 cm from isocenter to prevent patient-collimator collision during rotation. As seen in Figure 15 the electron arc collimating system consists of the x-ray jaws, the shaped secondary collimator, and the skin collimation. Note that the secondary collimator is trapezoidal in shape, its width being less for the superior chest wall anatomy, where the mean radius of curvature is less. This system assumes that the mean radius of curvature in any transverse plane of the patient (perpendicular to isocenter) is constant. If this is not the case, there can be some benefit in utilizing a dynamic multileaf secondary collimator (Leavitt et al., 1989).

More recently the question has been raised whether there is any benefit in using the x-ray multileaf collimator for electron collimation. Although the dose distribution can be made similar (Klein et al., 1996), a shorter SSD is required, resulting in its being a greater distance above the floor and hence being more difficult for patient setup using traditional techniques.

D. Collimator Leakage

Regardless of the collimating system, the dosimetric properties of the collimated beam and leakage must be understood. Obviously leakage occurs if the collimating material is too thin. Also, multiple scattering results in electrons traveling along curved, tortuous paths, so that it is possible for electrons to leak, even though the light field shows no direct leakage pathway. This was the case for some of the older Varian Clinac 1800 electron applicators (Keys and Purdy, 1984; Pennington et al., 1988), as shown in Figure 16. Lateral leakage through electron cones is also a concern, as shown by Hogstrom et al. (1985) and as illustrated in Figure 17. Therefore, it is recommended, that as part of acceptance testing, that leakage be measured perpendicular to central axis at the treatment SSD and that leakage perpendicular to the wall of any cone be measured.

V. Beam Monitoring

Beam monitoring is typically achieved through the use of dual, parallel plate, ionization chambers. The beam monitoring system is used for both x-ray and electron beams; however, the electron beam necessitates the use of "thin-window" chambers, otherwise the chambers generate excessive energy loss, increased bremsstrahlung dose, and excessive electron scattering, the latter resulting in a needless increase to the size of the virtual source. Therefore, transmission ionization chambers typically have thin Kapton windows onto which thin conducting gold foils are deposited. Some ionization chambers are sealed, and others are exposed to ambient atmosphere, requiring temperature-pressure correction.

The purpose of the dual ionization chambers is to monitor beam output, symmetry, and flatness. Dual chambers allow one chamber to be a primary output monitor and the other to serve as a redundant backup. Each chamber monitors symmetry and flatness in orthogonal directions. A typical system as found on the Varian Clinac 1800C is shown in schematic form in Figure 18. Note that symmetry is monitored by comparing ionization from two semi-circles and that flatness in monitored by comparing ionization collected by an inner circle and outer annulus.

VI. Conclusions

Electron beams with similar dosimetric properties are produced by a variety of different methods incorporated into the design of the electron beam treatment head. An understanding of the design of the electron beam treatment head is important in designing the appropriate dosimetry convention, in utilizing the appropriate dosimetry measurement methods, in establishing the appropriate quality assurance program, and in diagnosing machine failure that change dosimetric properties. As we look toward future, Monte Carlo methods of calculating electron beam dosimetry (Rogers et al., 1995) could become a new paradigm for machine commissioning. Such methods require a precise description of the phase space of the accelerated and bent electron beam and of the beam components in the treatment head.

REFERENCES

Boag J.W. The recombination correction for an ionization chamber exposed to pulsed radiation in a 'swept beam' technique. Phys. Med. Biol. 27:201-212, 1982.

Davis M.G., Nyerick C.E., Horton J.L., Hogstrom K.R. Use of routine quality assurance procedures to detect the loss of a linear accelerator primary scattering foil. Med. Phys. 23:521-522, 1996.

Ertan E., Muller-Sievers K., and Richl G. A new approach to overcome the inconveniences in electron dosimetry associated with the beam scanning technique in linacs. Phys. Med. Biol. 29:789-796, 1984.

Green A.D. Modeling of dual foil scattering systems for clinical electron beams, M.S. Thesis, The University of Texas Graduate School of Biomedical Sciences at Houston, 145 pp., 1991.

Hogstrom K.R., Meyer J.A., and Melson R. Variable electron collimator for the Mevatron 77: design and dosimetry. In: Proceedings of the 1985 Mevatron Users Conference, pp. 251-276, Iselin NJ; Siemens Medical Systems, 1985.

Hogstrom K.R. and Leavitt D. Dosimetry of electron arc therapy. In: H. Elson and C.†Born (eds.), Radiation Oncology Physics - 1986: Proceedings of the 1986 Summer School of the AAPM, pp. 265-295, New York; American Institute of Physics, 1987.

Hogstrom K.R., Kirsner S.M., Kurup R.G., Shiu A.S., and Moyers M.F. Operational characteristics of the Siemens Mevatron for electron arc beam. In: Proceedings of the 1987 Therapy Users Conference, pp. 185-214, Iselin, NJ; Siemens Medical Systems, 1987.

Hogstrom K.R., Boyer A.L., Shiu A.S., Ochran T.G., Kirsner S.M., Krispel F., and Rich†T. Design of metallic electron beam cones for an intraoperative therapy linear accelerator. International Journal of Radiation Oncology Biology Physics, 18:1223-1232, 1990.

Karzmark C.J. Advances in linear accelerator design for radiotherapy. Med. Phys. 11:105128, 1984.

Karzmark C.J., Nunan C.S., and Tanabe E. Medical electron accelerators. McGraw-Hill Inc., Health Professions Division, New York, 1993, 316 pp.

Keys R.A., and Purdy J.A. Radiation leakage from linac electron applicator assembly. Int. J. Radiat. Oncol. Biol. Phys. 10:713-721, 1984.

Khan F.M., Dopke K.P. Hogstrom K.R., Kutcher G.J., Nath R., Prasad S.C., Purdy J.A., Rozenfeld M., and Werner B.L. Clinical electron-beam dosimetry: Report of the AAPM radiation therapy committee task group 25. Medical Physics, 18:73-109, 1991.

Klein E.E., Li Z, and Low D. Feasibility study of multileaf collimated electrons with a scattering foil based accelerator. Radiother. Oncol. 41:189-196, 1996.

Leavitt D.D., Stewart J.R., Moeller J.H., Lee W.L., and Takach Jr. G.A. Electron arc therapy: Design, implementation, and evaluation of a dynamic multivane collimator system. Int. J. Radiat. Oncol. Biol. Phys. 17:1089-1094, 1989.

Leavitt D.D., Stewart J.R., Moeller J.H., and Earley L. Optimization of electron arc therapy doses by multi-vane collimator control. Int. J. Radiat. Oncol. Biol. Phys. 16:489-496, 1989.

Nyerick C.E., Ochran T.G., Boyer A.L., and Hogstrom K.R. Dosimetry characteristics of metallic cones for intraoperative radiotherapy. International Journal of Radiation Oncology Biology Physics, 21:501-510, 1991.

O'Brien P., Michaels H.B., Aldrich J.E., and Andrew J.W. Characteristics of electron beams from a 25-Mev linear accelerator. Med. Phys. 12:799-805, 1984.

Pennington E.C., Shirish L.K., and Wen B.-C. Leakage radiation from electron applicators on a medical accelerator. Med. Phys. 15:763-765, 1988.

Purdy C.J., Biggs P.J., Bowers C., Dally E., Downs W., Fraaes B.A., Karzmark C.J., Morgan P., Morton R., Palta J., Rosen I.I., Thorson T., Svensson G., and Ting J. Medical accelerator safety considerations: Report of AAPM Radiation Therapy Committee Task Group No. 35. Med. Phys. 20:1261-1275, 1993.

Rogers D.W.O., Faddegon B.A., Ding G.X., Ma C.M., We J., and Mackie T.r. BEAM: A Monte Carlo code to simulate radiotherapy treatment units. Med. Phys. 22:503-524, 1995.

GL:H:\Gwen\Manuscript\Elecbeamtreatmenthead.Doc:09/22/97 8:13 PM

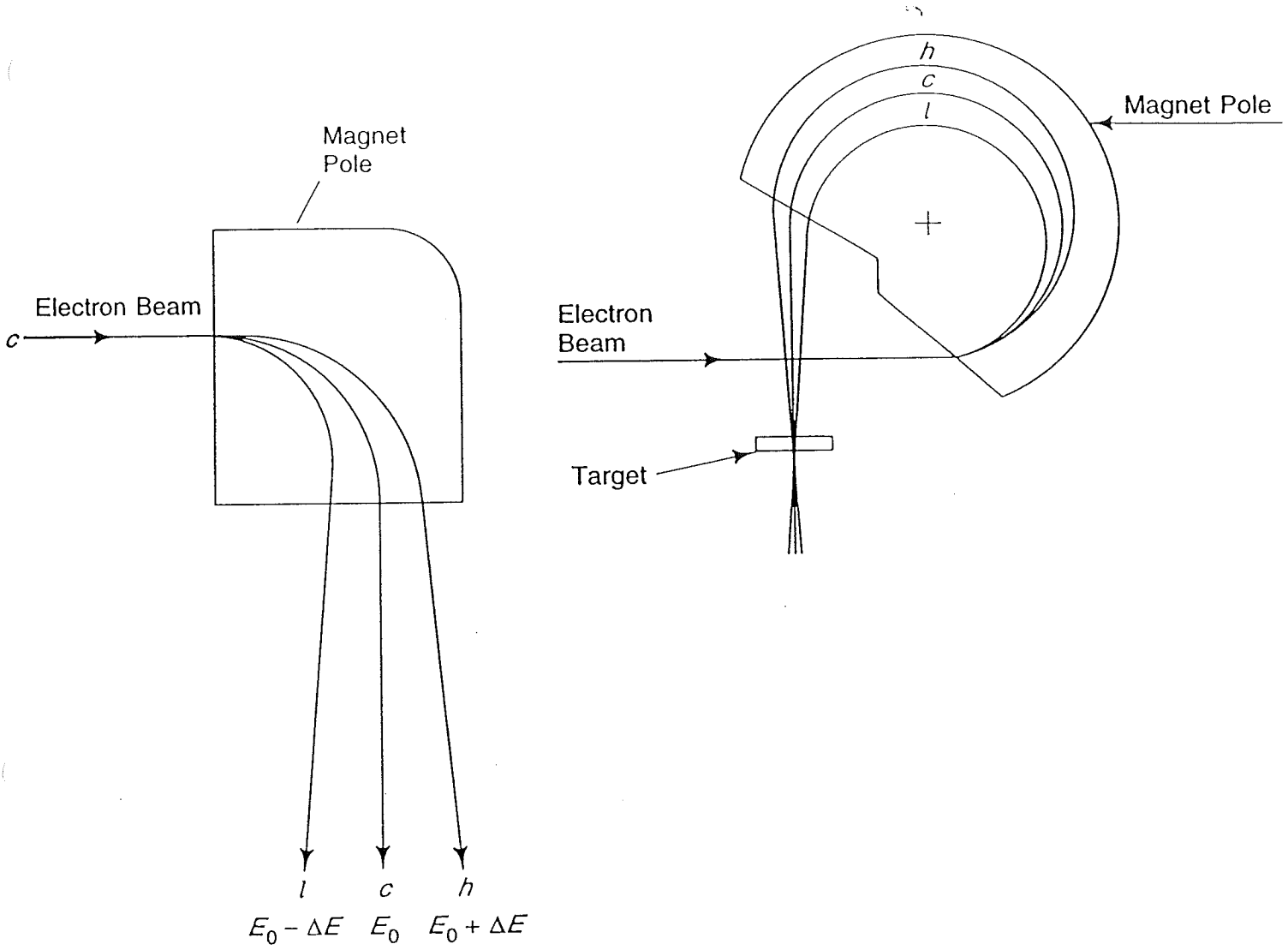

Figure 1: (a) 90° bending magnet creates energy dispersion, which is not suitable for an electron therapy beam. (b) 270° bending magnet focuses high (h), central (c), and low (l) energy electrons back to a common point. This creates an energy-angle correlation, which is still not suitable for electron therapy. (from Karzmark et al., 1993)

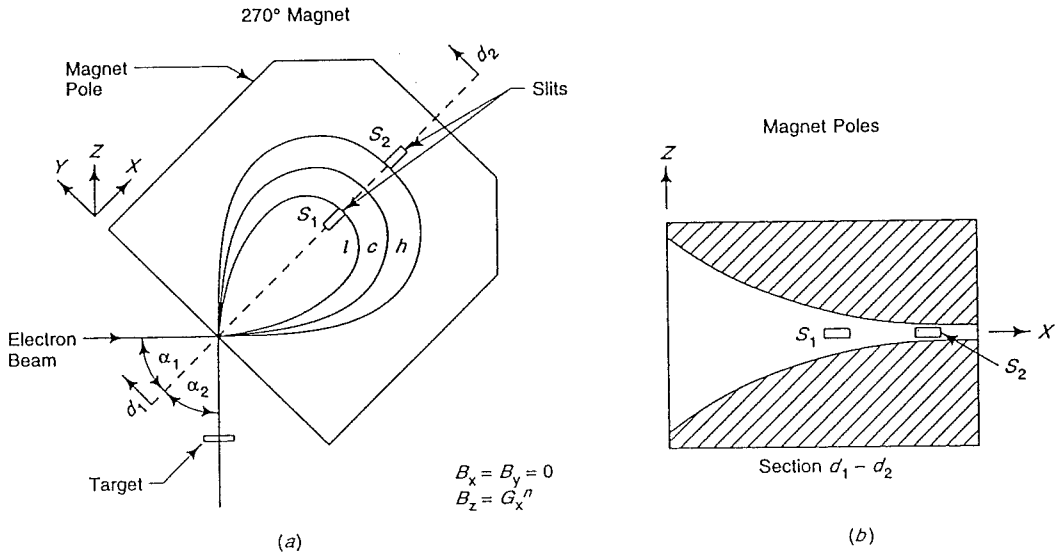

Figure 2: Earliest concept of an achromatic bending magnet, referred to as a magnetic mirror, was proposed by Enge. (a) The trajectories of the high (h), central (c), and low (l) energy electrons return to the same point with the same direction. (b) The achromatic bending magnet results from approximately hyperbolic pole contours. (from Karzmark et al., 1993)

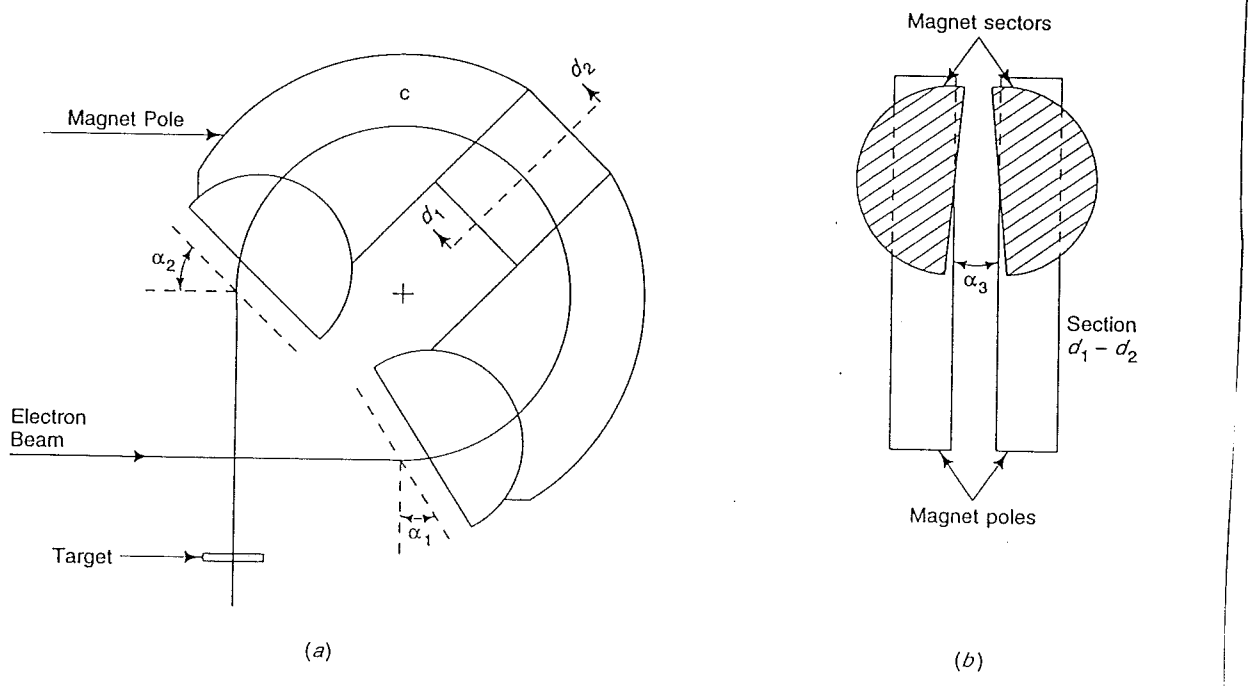

Figure 3: Another 270° achromatic bending magnet, the type employed by the Siemens Mevatron. (a) The 270° bending magnet has adjustable input and output pole faces. It has a constant magnetic field except for the mid-arc region. (b) Cross-section of adjustable tilted pole gap. (from Karzmark et al., 1993)

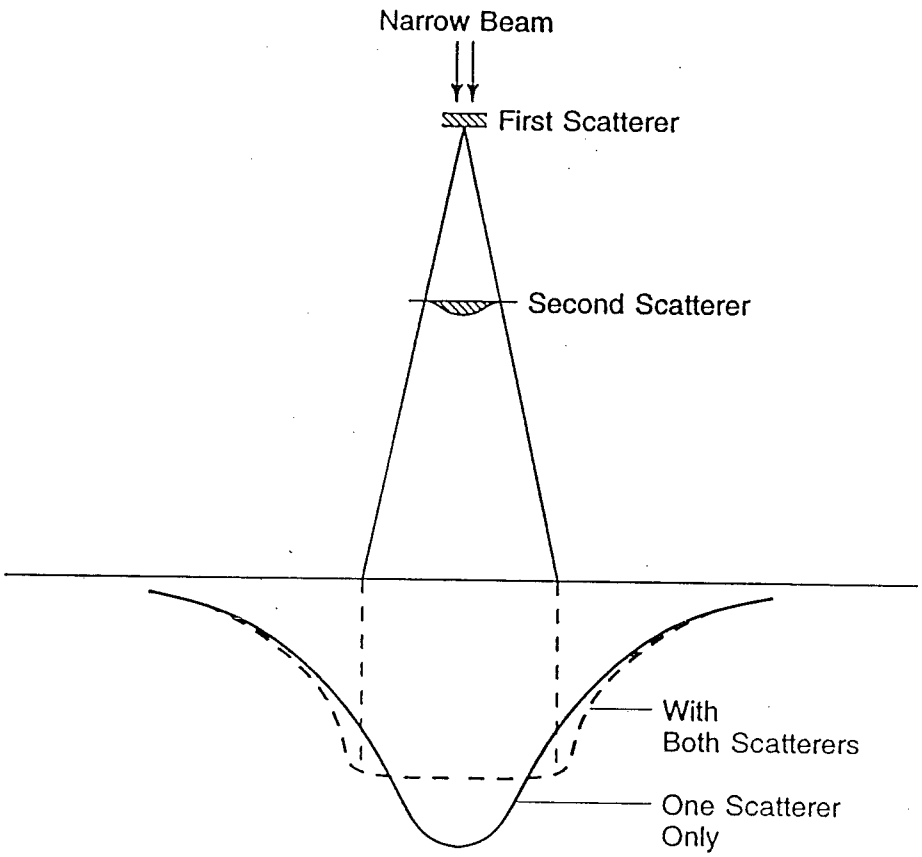

Figure 4: Cross-section of electron beam dual scattering foil system. If only the primary foil (first scatterer) is present, the resulting beam profile at isocenter is Gaussian. The addition of a Gaussian-shaped secondary foil (second scatterer) produces a more uniform beam profile at isocenter. (from Karzmark et al., 1993)

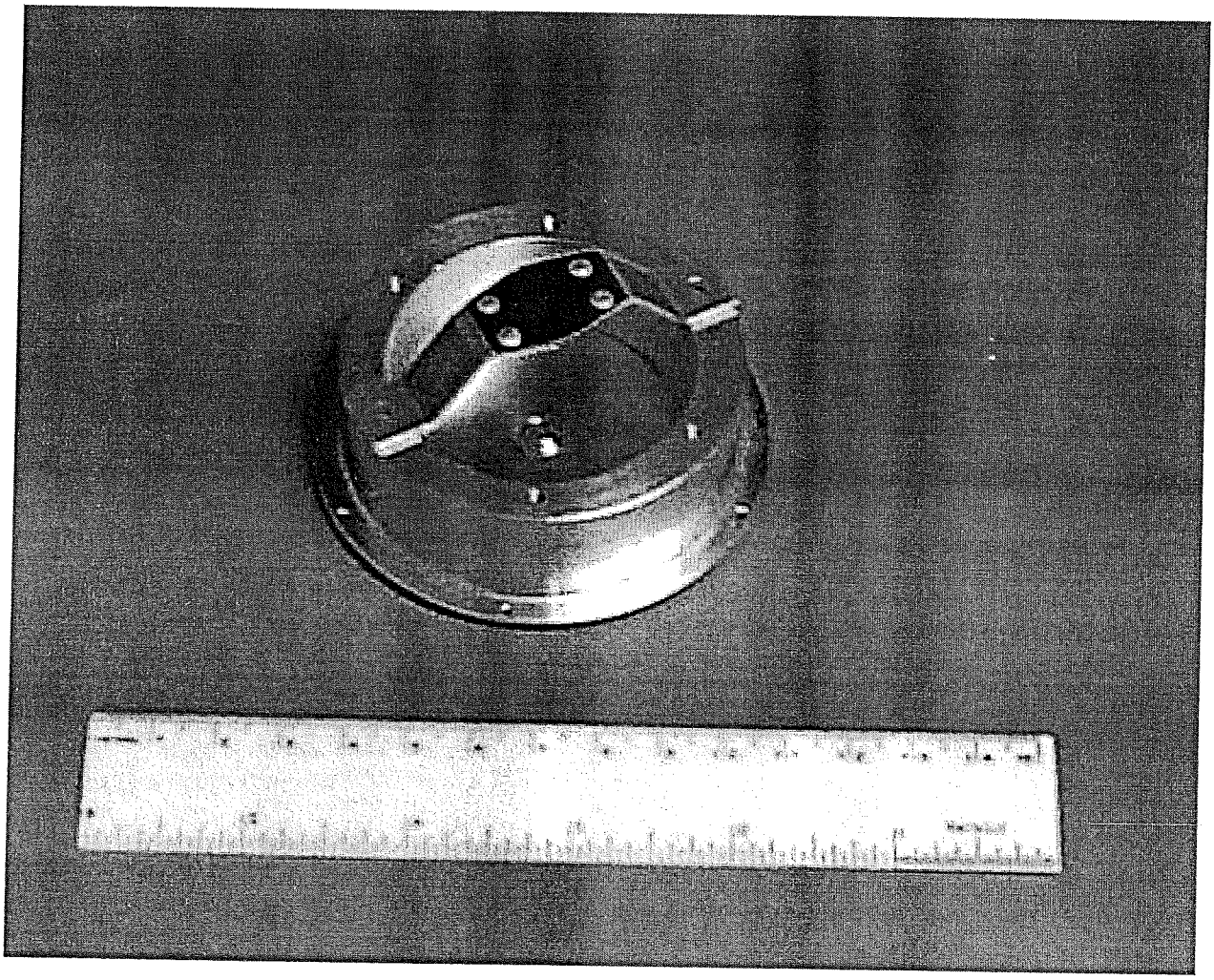

Figure 5: Primary and secondary scattering foil unit for the Varian Clinac 2100C. Note the constant thickness primary foil on top and the stepped secondary foil mounted to the bottom plate.

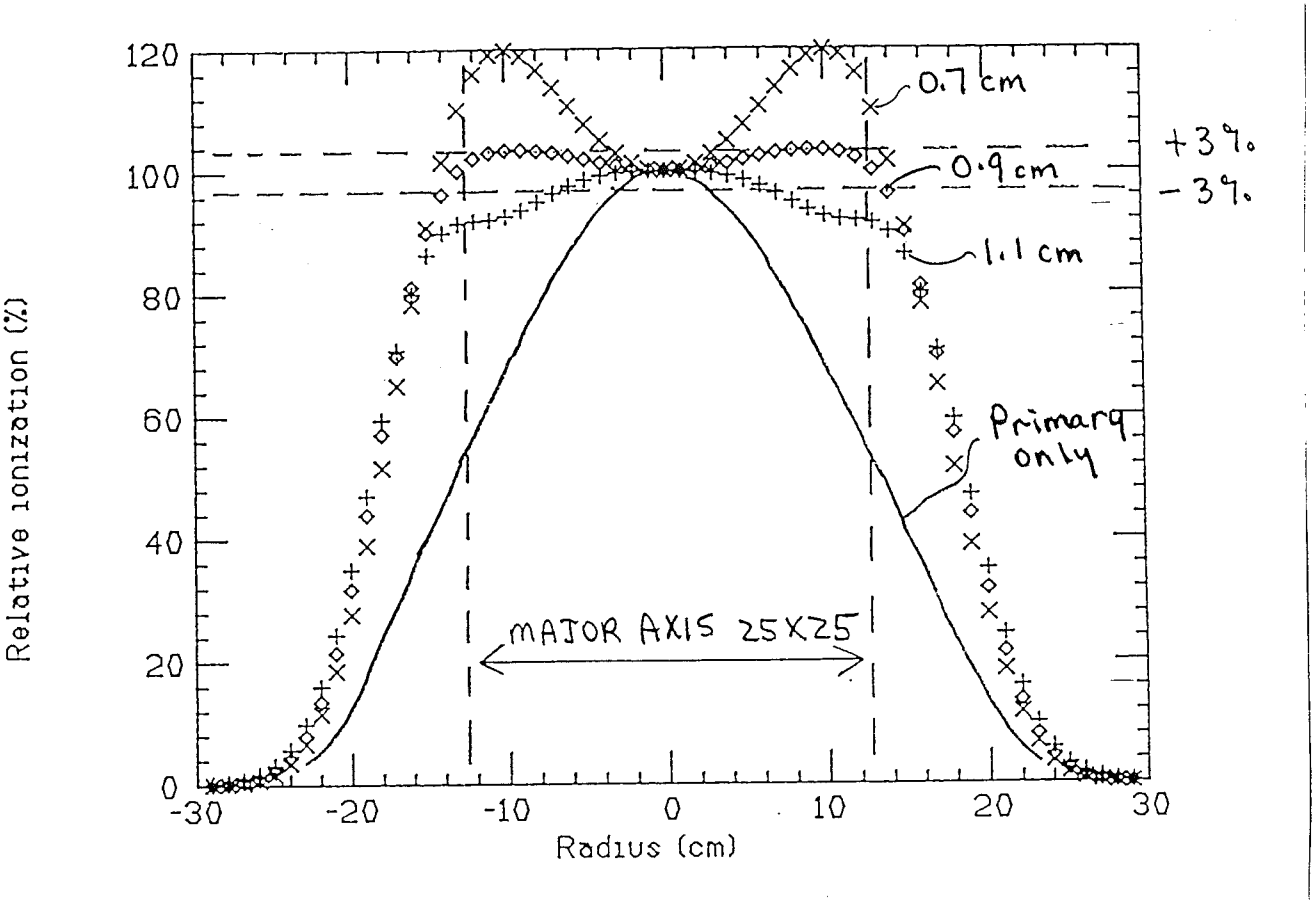

Figure 6: Comparison of beam flatness for a 12-MeV beam, which has a 0.0036-cm Au primary foil, and no secondary foil with Gaussian-shaped secondary foils (central thickness = 0.13 cm Al; rms equals 0.7, 0.9, and 1.1 cm). (from Green, 1991)

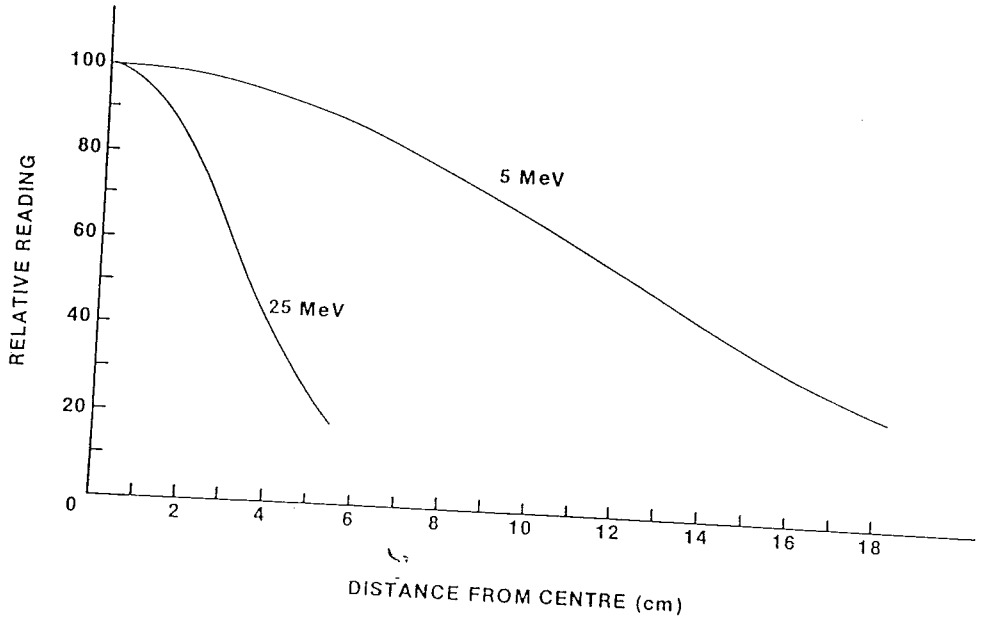

Figure 7: Radial profiles of the unscanned electron beams for the AECL Therac-25 5- and 25-MeV beams. (from O'Brien et al., 1985)

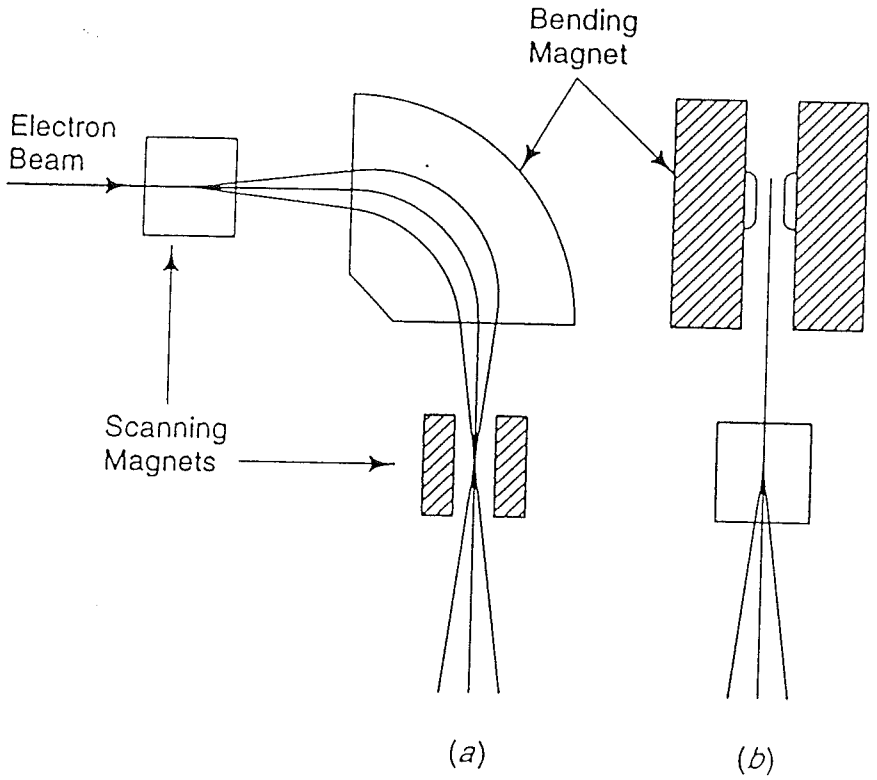

Figure 8: Orthogonal views of orthogonal scanning magnets before and after a 90° bending magnet, (a) in the bend plane and (b) orthogonal to bend plane. (from Karzmark et al., 1993)

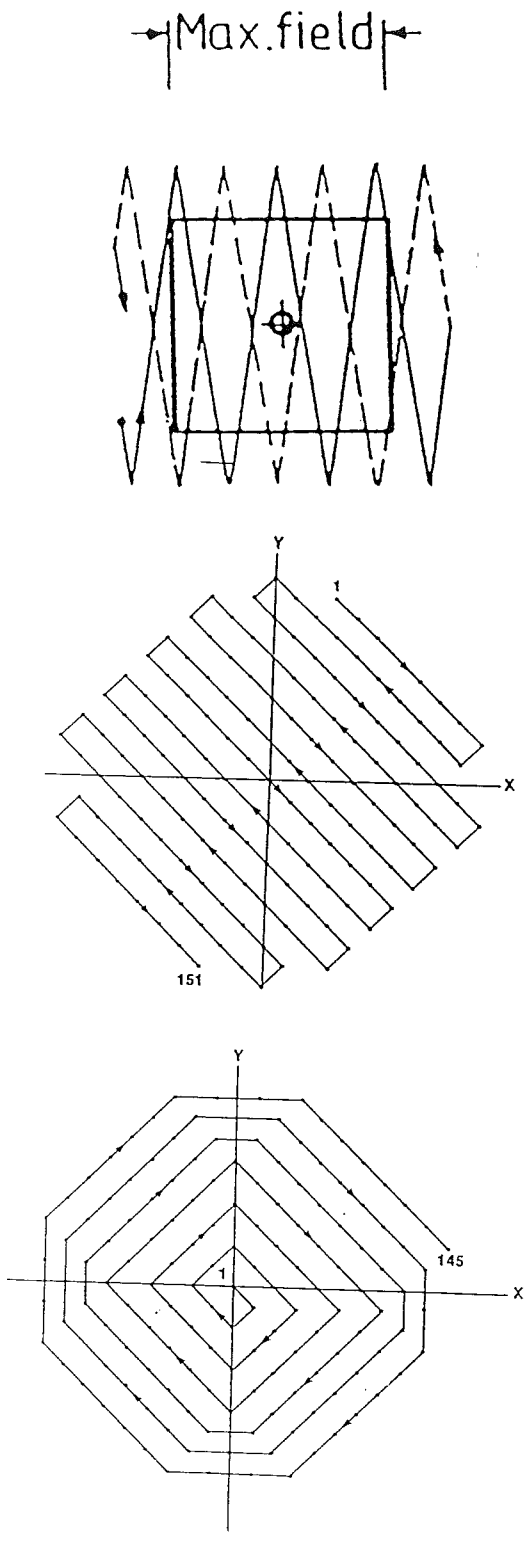

Figure 9: Beam scanning patterns. Top figure illustrates asynchronous raster scanning employed on the AECL Therac 20. The width of the square is $\sqrt{2}$ times 30 cm, the diagonal length of the largest field size. (from Ertan et al., 1984) The middle (raster) and lower (spiral) scan patterns are repetitive and are used for the high-energy and low-energy beams respectively of the AECL Therac 25. (from O'Brien et al., 1985)

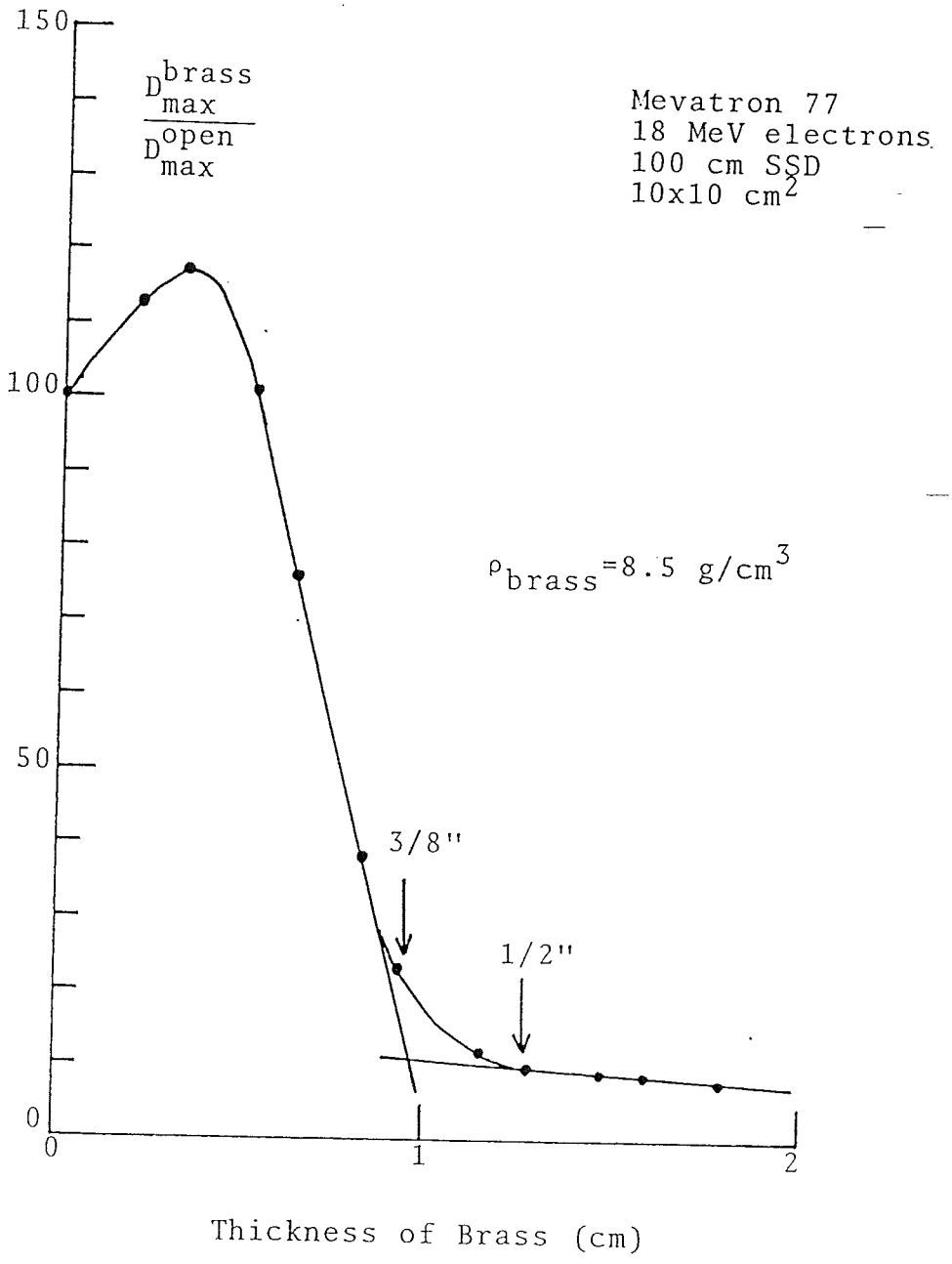

Figure 10: Transmission curve in brass for 18-MeV electron beam shows 0.5" of brass stops all primary electrons. (from Hogstrom et al., 1985)

ELECTRON COLLIMATOR DESIGN CONCEPT

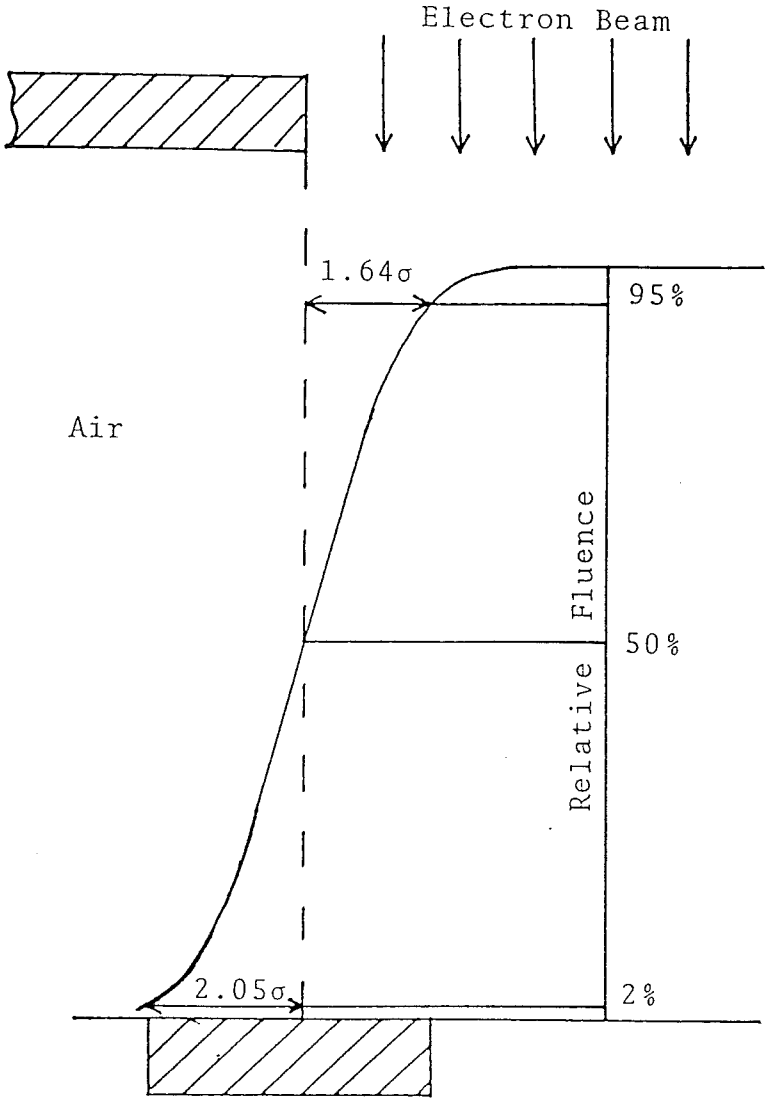

Figure 11: Electron collimating concept shows that the downstream collimator should be designed to intercept penumbra cast by upstream collimator. (from Hogstrom et al., 1985)

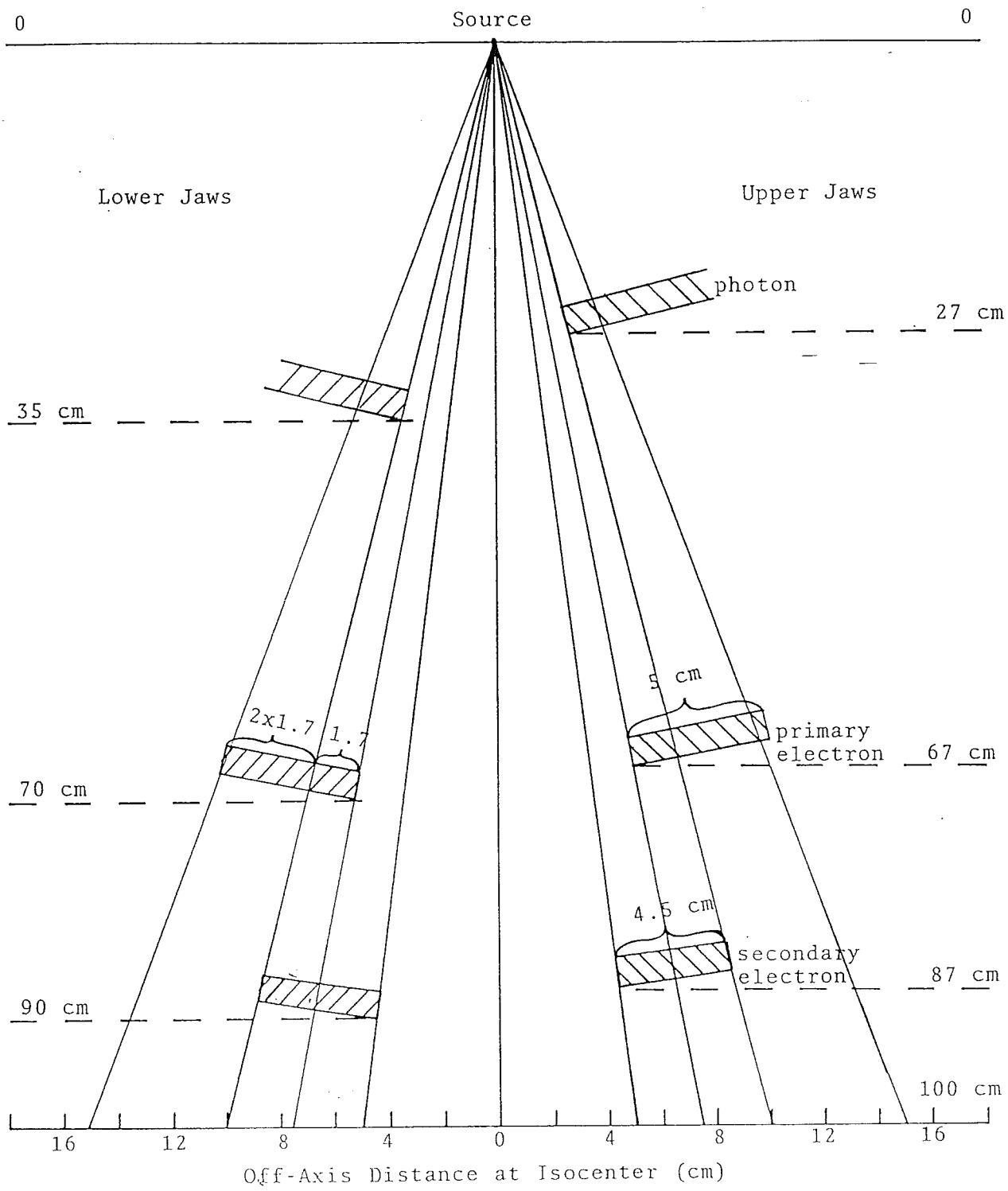

Figure 12: Schematic of geometry for Siemens Mevatron variable electron collimator. Each half represents orthogonal axes. (from Hogstrom et al., 1985).

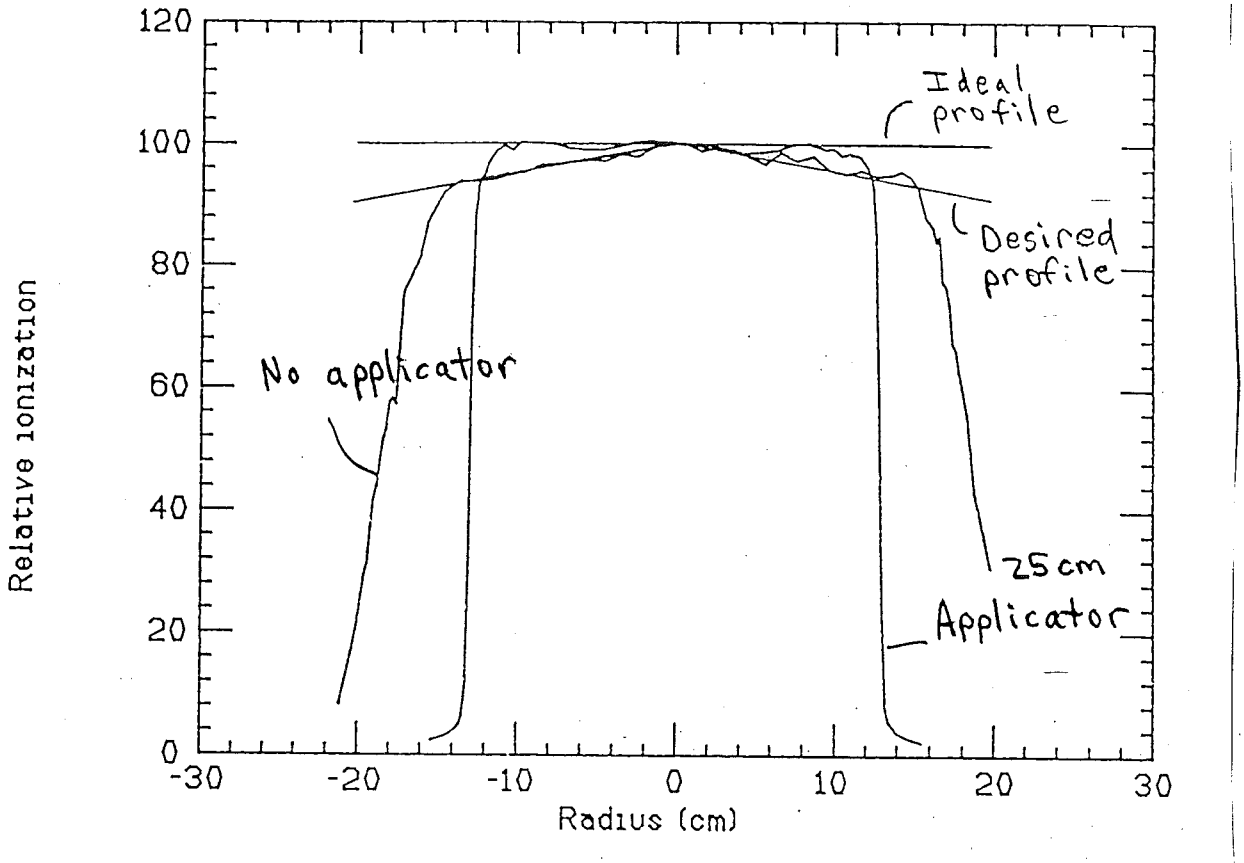

Figure 13: Beam profiles with and without the 25×25 cm^2 applicator present are compared for a Siemens Mevatron 20-MeV beam. (from Green, 1991)

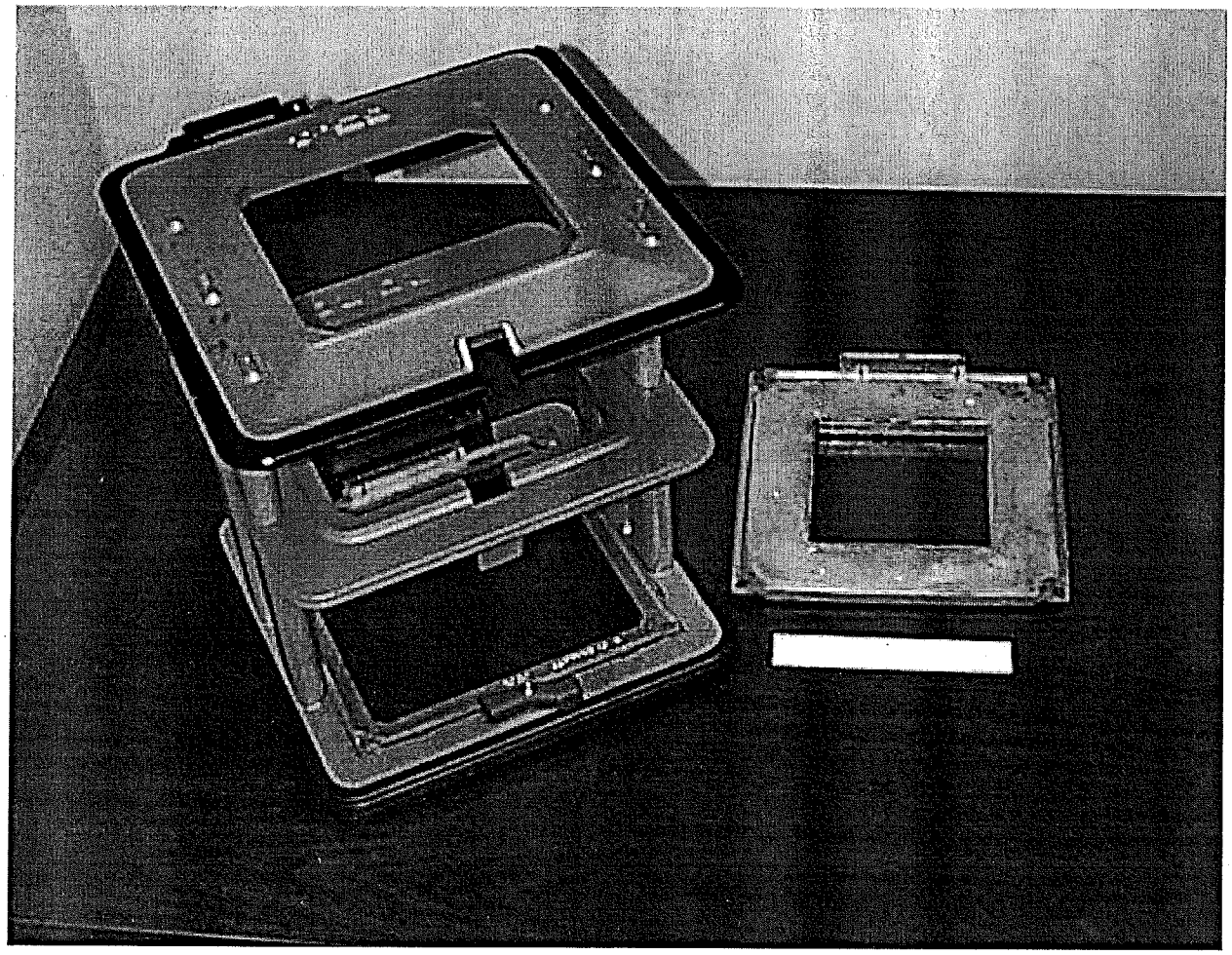

Figure 14: Electron applicator (20 x 20 cm^2) with a 12.5 x 12.5 cm^2 Cerrobend insert. Note the removal clip. To the right is a blank frame in which Cerrobend inserts fit. Note the coding system on the perimeter which is used for patient insert identification. (Varian Clinac 2100C)

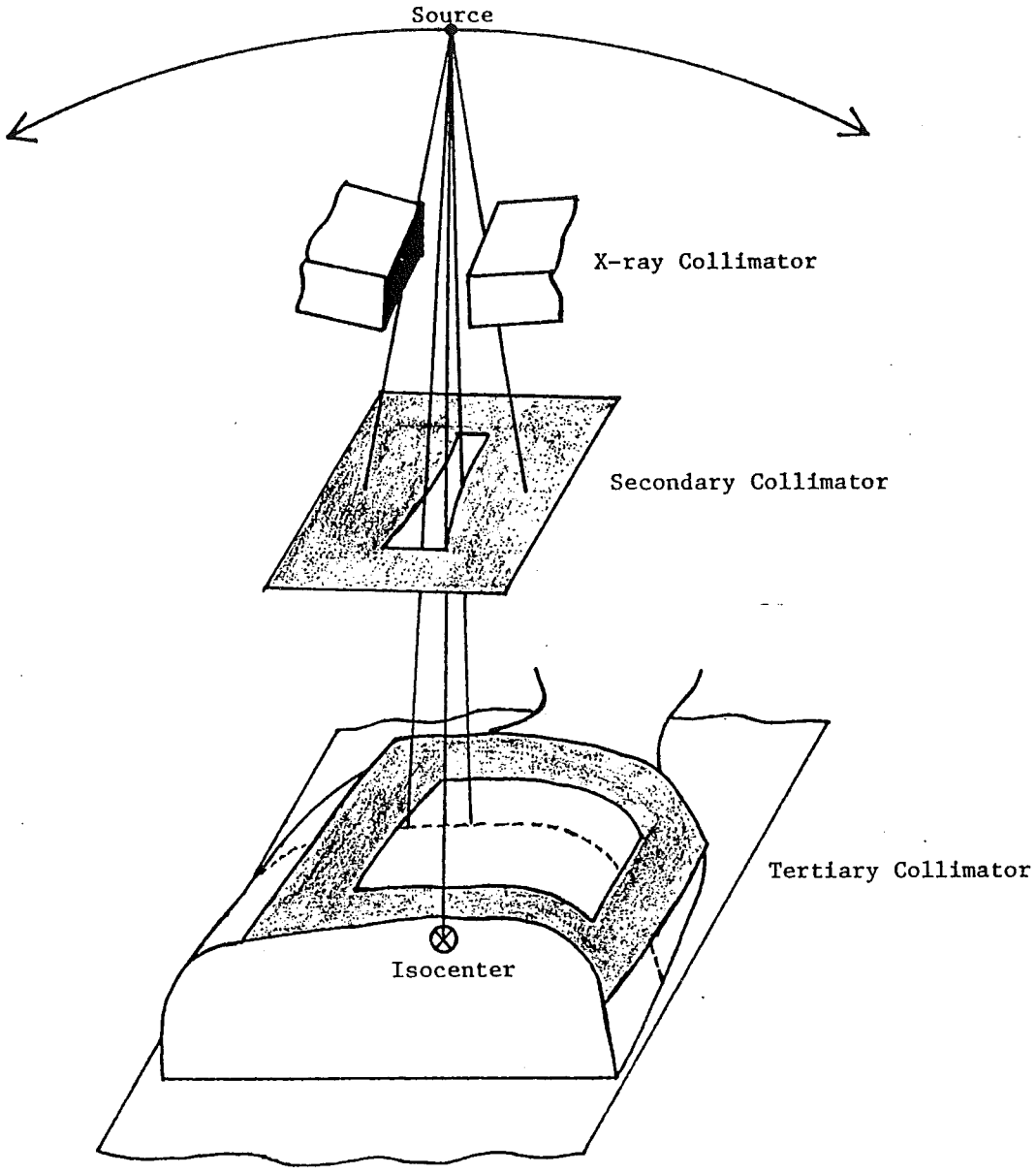

Figure 15: Electron arc collimating system showing three levels of collimation: x-ray jaws, secondary custom Cerrobend insert, and tertiary skin collimation. (from Hogstrom and Leavitt, 1987)

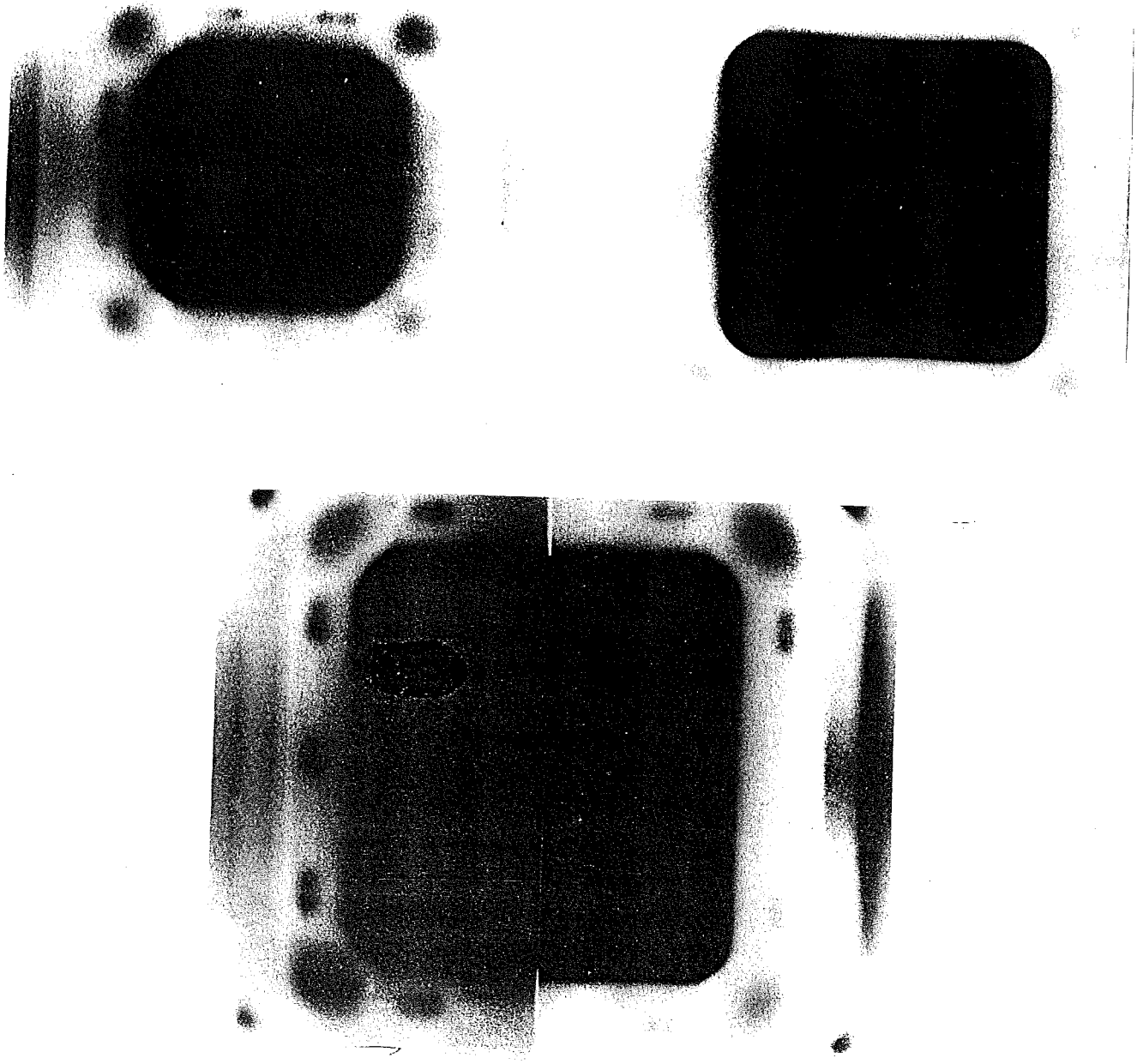

Figure 16: X-ray films taken at 100 SAD indicate the areas of leakage radiation for the 15 x 15 cm^2, 20 x 20 cm^2 and 25 x 25 cm^2 applicators. The gantry is to the right for each film. (Varian Clinic 20/20MeV) (from Keys and Purdy, 1998)

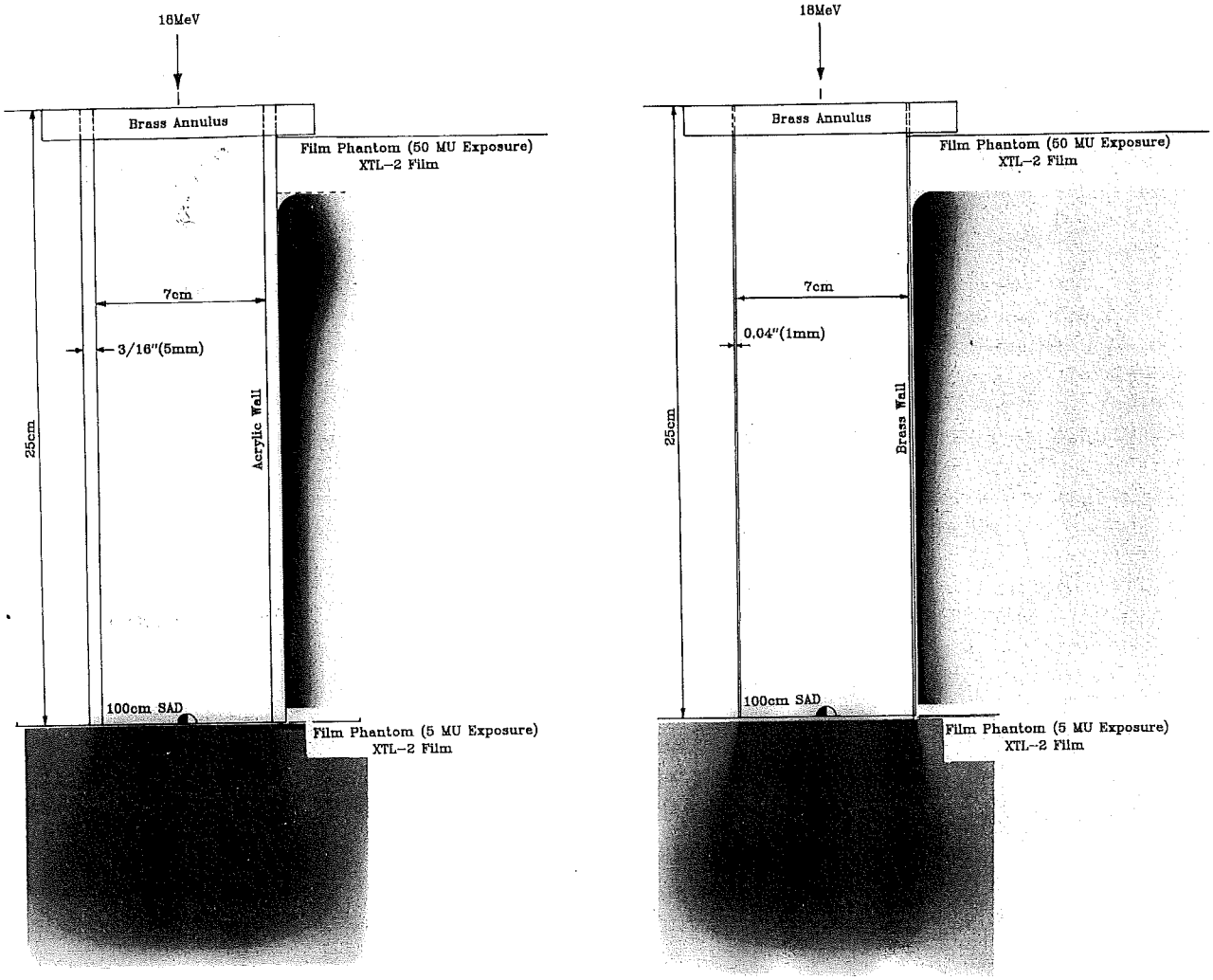

Figure 17: Example of electron leakage through lateral walls of intraoperative electron therapy cones made of 5 mm acrylic and 1 mm brass. (from Hogstrom et al., 1990)

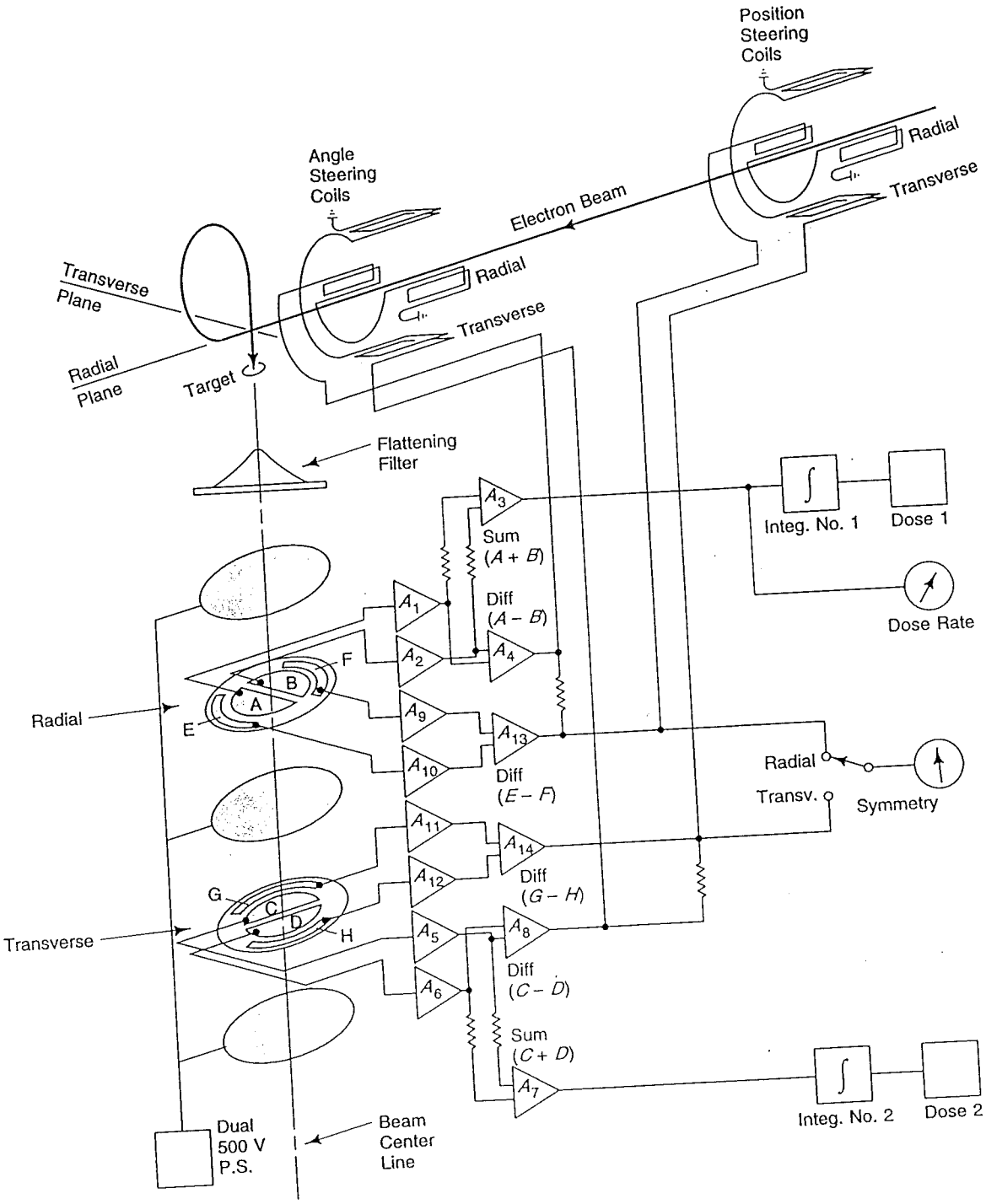

Figure 18: Schematic of dual transmission ionization chamber system, which can monitor beam output, flatness, and symmetry. (from Karzmark et al., 1993)